

## ULTIMATE STRENGTH OF PIPE COLUMNS WITH INITIAL CURVATURE

*By Tongchat HONGLADAROMP\**, *Somchet TAERACOOP\*\**, *Fumio NISHINO\*\*\**  
*and Seng-Lip LEE\*\*\*\**

### 1. INTRODUCTION

Thin wall tubular columns normally have sufficiently small diameter to thickness ratio so that local buckling will not occur. The column strength, however, is influenced by some unavoidable imperfection in manufacturing and construction such as initial crookedness and eccentricity of loading. The initial crookedness reduces the strength of the column and hence its effect should be thoroughly investigated.

The strength of eccentrically loaded columns was investigated by Karman<sup>1)</sup>, Baker, Horne and Roderick<sup>2)</sup>, Galambos and Ketter<sup>3)</sup> and many other investigators. Horne<sup>4)</sup>, in studying the strength of rectangular columns, presented a stability criterion which was later used by several investigators<sup>5),6),7)</sup>. Recently, the effect of initial imperfection on the strength of axially loaded columns was studied by Batterman and Johnston<sup>8)</sup> while Rossow, Barney and Lee<sup>9)</sup> studied the effect on eccentrically loaded wide flange columns. The strength of elastic-perfectly plastic tubular columns without imperfection was investigated by Snyder and Lee<sup>10)</sup> who also employed the criterion developed by Horne.

In the present study of elastic-perfectly plastic

tubular columns with initial imperfection subjected to asymmetrical loading, the technique of Snyder and Lee<sup>10)</sup> is used to determine the envelope of equilibrium curves from which the column curves are constructed. The initial imperfection or the crookedness of the column is considered in the form of initial curvature which is kept constant throughout the length. The effect of shear stresses on yielding, residual stresses and stress reversal are not considered.

### 2. PROPERTIES OF PIPE COLUMNS

#### (1) Moment-Thrust-Curvature Relationships

In the following analysis, the moment  $M$ , thrust  $P$  and curvature will be nondimensionalized in the form

$$m = \frac{M}{M_0} \dots\dots\dots(1)$$

$$p = \frac{P}{P_0} \dots\dots\dots(2)$$

$$\phi = \frac{\Phi}{\epsilon_0/a} \dots\dots\dots(3)$$

in which

$$M_0 = 4a^2h\sigma_0 \dots\dots\dots(4)$$

$$P_0 = 2\pi ah\sigma_0 \dots\dots\dots(5)$$

In these equations,  $\epsilon_0$  is the strain at yield point,  $a$  the mean radius of the tubular column section,  $h$  the thickness,  $\sigma_0$  the yield stress and  $M_0$  and  $P_0$  are the fully plastic moment and normal force of the pipe section respectively.

The moment-thrust-curvature relationships of the pipe column section, when subjected to bending and axial force, can be written in the following nondimensional forms depending on the three stress distributions as shown in Fig. 1.

*Elastic Case:* Referring to Fig. 1 (b), the moment, thrust and curvature are related by two positive constants  $c$  and  $t$  in the parametric form

\* Ph.D., Assistant Professor of Civil Engineering, Asian Institute of Technology, Bangkok, Thailand.  
 \*\* M. Eng., Engineer, National Economic Development Board, Bangkok, Thailand.  
 \*\*\* Ph.D., Associate Professor of Civil Engineering, Asian Institute of Technology, Bangkok, Thailand; on leave from University of Tokyo, Japan.  
 \*\*\*\* Ph.D., Professor and Chairman, Structural Engineering and Mechanics Division, Asian Institute of Technology, Bangkok, Thailand.

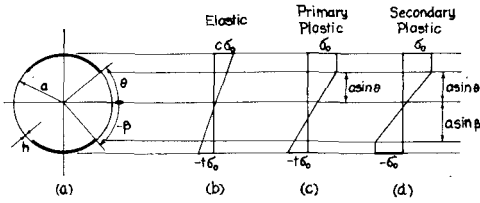


Fig. 1 Cross Section and Stress Distributions.

$$m = \frac{\pi(c+t)}{8} \dots\dots\dots(6)$$

$$p = \frac{c-t}{2} \dots\dots\dots(7)$$

$$\phi = \frac{c+t}{2} \dots\dots\dots(8)$$

*Primary Plastic Case:* For the stress distribution shown in Fig. 1 (c), the moment-thrust-curvature relationships are related in terms of the two parameters  $t$  and  $\theta$  by

$$m = \frac{1+t}{4(1+\sin \theta)} \left[ \sin \theta \cos \theta + \theta + \frac{\pi}{2} \right] \dots\dots\dots(9)$$

$$p = 1 - \frac{1+t}{\pi(1+\sin \theta)} \left[ \left( \theta + \frac{\pi}{2} \right) \sin \theta + \cos \theta \right] \dots\dots\dots(10)$$

$$\phi = \frac{1+t}{1+\sin \theta} \dots\dots\dots(11)$$

in which  $\theta$  is positive when measured counterclockwise from the horizontal axis.

*Secondary Plastic Case:* For the stress distribution shown in Fig. 1 (d), the nondimensional moment, thrust and curvature can be written in the form

$$m = \frac{\sin \theta \cos \theta - \sin \beta \cos \beta + \theta - \beta}{2(\sin \theta - \sin \beta)} \dots\dots(12)$$

$$p = \frac{2(\beta \sin \beta - \theta \sin \theta + \cos \beta - \cos \theta)}{\pi(\sin \theta - \sin \beta)} \dots\dots\dots(13)$$

$$\phi = \frac{2}{\sin \theta - \sin \beta} \dots\dots\dots(14)$$

in which  $\theta$  and  $\beta$  are the two parameters, being positive when measured counterclockwise from the horizontal axis. It should be noted that the angle  $\beta$  shown in Fig. 1 (d) is negative by definition.

For the elastic case, eliminating  $c$  and  $t$  between Eqs. (6) and (8) leads to the linear moment-curvature relationship

$$\phi = \frac{4m}{\pi} \dots\dots\dots(15)$$

In each of the plastic cases, the two parameters

can be solved numerically from the two transcendental equations for given values of  $m$  and  $p$ . The curvature is then determined by substituting the results into either Eqs. (11) or (14).

(2) **Boundary of Stress Zones**

The boundary between the elastic and primary plastic zones represented by the straight line  $ac$  in Fig. 2 can be determined from

$$m = \frac{\pi}{4}(1-p) = m_e \dots\dots\dots(16)$$

and the boundary between the primary and secondary plastic zones, indicated by the curve  $ab$ , can be obtained from

$$m = \frac{\sin \theta \cos \theta + \theta + \frac{\pi}{2}}{2(1+\sin \theta)} = m_p \dots\dots\dots(17)$$

$$p = 1 - \frac{2 \left[ \left( \theta + \frac{\pi}{2} \right) \sin \theta + \cos \theta \right]}{\pi(1+\sin \theta)} \dots\dots\dots(18)$$

When  $\theta$  approaches  $\beta$ , i.e., when the entire section becomes plastic, the outer boundary of the secondary plastic zone, represented by the curve  $ab$ , can be shown to be

$$m = \cos \beta = \bar{m} \dots\dots\dots(19)$$

$$p = -\frac{2\beta}{\pi} = -\frac{2}{\pi} \cos^{-1} \bar{m} \dots\dots\dots(20)$$

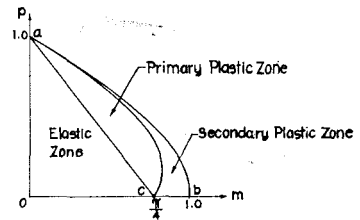


Fig. 2 Boundary of Stress Zones

3. **GOVERNING EQUATIONS AND INTEGRATION SCHEME**

(1) **The Governing Equations**

The problem of eccentrically loaded pipe columns can be treated by considering the cantilever column subjected to axial force  $P$ , transverse shear force  $Q$  and bending moment  $M$  at the free end as shown in Fig. 3. Initial imperfection is characterized by constant initial curvature throughout the length of the column. The equilibrium condition and the curvature-displacement relation, in accordance with the small deflection theory, are given by

$$M = M_f - (PY + QX) \dots\dots\dots(21)$$

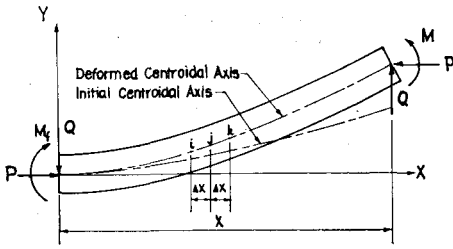


Fig. 3 Cantilever Column with Initial Curvature.

$$\frac{d^2 Y}{dX^2} = \phi + \phi_0 \quad \dots\dots\dots(22)$$

where  $M_f$  is the fixed end moment,  $X$  the length of the cantilever column,  $Y$  the transverse deflection, and  $\phi$  and  $\phi_0$  are the curvature due to bending and the initial curvature respectively.

Introducing the following nondimensionalization,

$$x = \frac{X}{a} \sqrt{\epsilon_0} \quad \dots\dots\dots(23)$$

$$y = \frac{Y}{a} \quad \dots\dots\dots(24)$$

$$q = \frac{Q}{P_0 \sqrt{\epsilon_0}} \quad \dots\dots\dots(25)$$

Eqs. (21) and (22), in view of Eqs. (1) to (5), reduce to the form

$$m = m_f - \frac{\pi}{2} (py + qx) \quad \dots\dots\dots(26)$$

$$\frac{d^2 y}{dx^2} = \phi + \phi_0 \quad \dots\dots\dots(27)$$

in which  $m_f = M_f/M_0$  and  $\phi_0$  is the nondimensional initial curvature which can be expressed in terms of the initial radius of curvature  $\rho_0$  as

$$\phi_0 = \frac{a}{\epsilon_0 \rho_0} \quad \dots\dots\dots(28)$$

The differential equation, Eq. (27), is the governing equation for all cases provided that the appropriate expression for the curvature, either Eqs. (8), (11) or (14), is used.

In the elastic zone, substituting Eq. (26) into Eq. (15) and the result into Eq. (27) leads to

$$y'' + 2py = \frac{4m}{\pi} f - 2qx + \phi_0 \quad \dots\dots\dots(29)$$

in which prime denotes differentiation with respect to  $x$ . Solving Eq. (29) with the boundary conditions at the fixed end,  $y(0) = 0$  and  $y'(0) = 0$ , leads to the solution

$$y = \frac{q}{p \sqrt{2p}} \sin(\sqrt{2p} x) - \left( \frac{2m_f}{\pi p} + \frac{\phi_0}{2p} \right)$$

$$\times \cos(\sqrt{2p} x) + \left( \frac{2m_f}{\pi p} + \frac{\phi_0}{2p} \right) - \frac{q}{p} x \quad \dots\dots\dots(30)$$

Substituting Eq. (30) into Eq. (26) yields

$$m = \left( m_f + \frac{\pi}{4} \phi_0 \right) \cos(\sqrt{2p} x) - \frac{\pi q \sin(\sqrt{2p} x)}{2\sqrt{2p}} - \frac{\pi}{4} \phi_0 \quad \dots\dots\dots(31)$$

In the two plastic zones, the governing differential equations are nonlinear and the following numerical integration technique is used to obtain the solutions.

(2) Numerical Integration

Consider the deformed segment  $ijk$  of the column shown in Fig. 3, the curvature at the pivot point  $j$  can be written in the central difference form as

$$y_j'' = \frac{1}{(\Delta x)^2} (y_k - 2y_j + y_i) \quad \dots\dots\dots(32)$$

from which

$$y_k = y_j'' (\Delta x)^2 + 2y_j - y_i \quad \dots\dots\dots(33)$$

where, in view of Eq. (27),

$$y_j'' = \phi_j + \phi_0 \quad \dots\dots\dots(34)$$

At the pivot point  $j$ , the moment  $m$  can be determined from Eq. (26) for particular values of  $p$ ,  $q$ ,  $\phi_0$  and  $m_f$  which may assume the value in the range  $-m \leq m_f \leq m$ . The curvature  $\phi_j$  can then be obtained from the appropriate equations corresponding to its stress zone as previously described. The deflection  $y_k$  thus can readily be determined from Eq. (33) in view of Eq. (34) and the deflections at point  $i$  and  $j$  which are obtained in the preceding calculations. The integration process starts from the fixed end where  $j=1$  at which  $y_j=0$  and  $y_i=y_k$ . Then the calculation can proceed for  $j=2, 3, 4, \dots$ .

4. EQUILIBRIUM CURVES AND STABILITY CRITERION

(1) Envelope of Equilibrium Curves

For a set of  $p$ ,  $q$  and  $\phi_0$  and various assumed values of  $m_f$ , the  $m-x$  relationships can be determined, with the aid of the numerical integration technique, and plotted as shown in Fig. 4 (a). These  $m-x$  curves are referred to as equilibrium curves. When the column is entirely elastic, the equilibrium curves will pass through a fixed point  $(x^*, m^*)$  regardless of the assumed value of  $m_f$ . The point  $(x^*, m^*)$  is governed by the

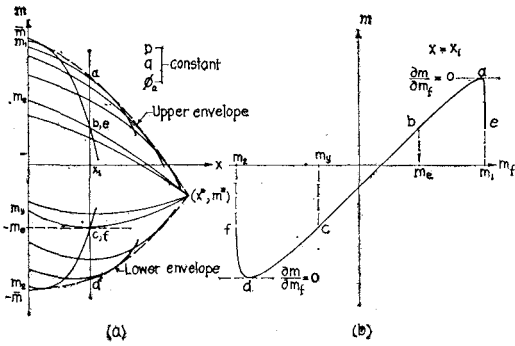


Fig. 4 Equilibrium Curves and Stability Criterion.

non-dimensional Euler length

$$x = x^* = \frac{\pi}{2\sqrt{2p}} \dots\dots\dots(35)$$

and the corresponding moment, obtained by substituting  $x^*$  in Eq. (31).

$$m = m^* = -\frac{\pi q}{2\sqrt{2p}} - \frac{\pi}{4} \phi_0 \dots\dots\dots(36)$$

Applying Horne's stability criterion<sup>4)</sup>, the envelope of the equilibrium curves can be constructed as indicated by the dotted curves in Fig. 4 (a). The envelope is the boundary of the stable equilibrium domain of the cantilever columns.

(2) Limitations on Shear Forces

The relation between  $p$  and  $q$  in the elastic zone can be found by equating  $m^*$  from Eq. (36) to the negative value of  $m_e$  in Eq. (16) which yields

$$q = q^* = \frac{(1-p-\phi_0)\sqrt{2p}}{2} \dots\dots\dots(37)$$

When  $q \leq q^*$ , the entire column will be elastic for  $m_y \leq m_f \leq m_e$  where

$$m_y = -\frac{\pi}{2} \sqrt{\left[\frac{(1-p)}{2} - \frac{\phi_0}{2}\right]^2 - \frac{q^2}{2p}} - \frac{\pi}{4} \phi_0 \dots\dots\dots(38)$$

is the value of  $m_f$  which causes initial yielding somewhere in the column. The maximum statically admissible value of  $q$  is approximately obtained from Eqs. (19) and (36), in view of Eq. (20), by eliminating  $m$ , yielding

$$q = q^{**} = \frac{2\sqrt{2p}}{\pi} \left[ \cos\left(-\frac{\pi}{2} p\right) - \frac{\pi}{4} \phi_0 \right] \dots\dots\dots(39)$$

The relation between  $q$  and  $p$  given by Eqs. (37) and (39) are plotted in Fig. 5 for  $\phi_0 = 1/12$

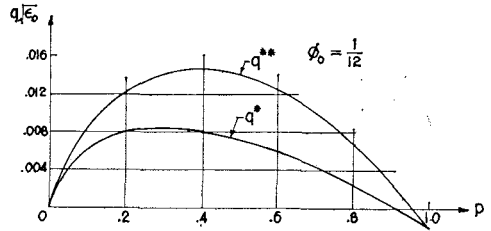


Fig. 5 Limitation on  $q$

for illustration. These relationships are used in selecting the parameters  $p$  and  $q$  in this study. It should be pointed out that when  $q$  assumes values close to  $q^{**}$ , the calculations become very sensitive.

5. NUMERICAL RESULTS

(1) Construction of Column Curves

In the determination of the ultimate strength of simply supported pipe columns subjected to asymmetrical loading with  $-1 \leq \kappa \leq 1$  as shown in Fig. 6, it is more useful to present the strength of the column in the form of conventional col-

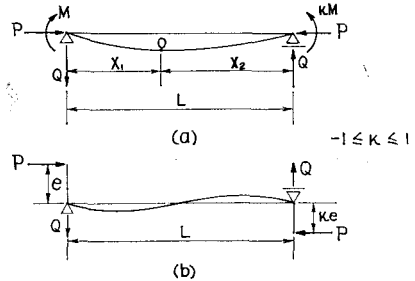


Fig. 6 Simply Supported Columns

umn curves. The column can be treated as two cantilever columns of length  $X_1$  and  $X_2$  with the fixed end at point 0 as shown in Fig. 6 (a). The segment to the right of point 0 is subjected to the same loading as the cantilever column of Fig. 3, while the shear force  $Q$  acting on the segment to the left of point 0 is in the opposite direction for which care should be exercised in using the appropriate envelopes. A typical envelope for the whole column constructed for particular values of  $q\sqrt{\epsilon_0}$  and  $\phi_0$  versus various magnitude of  $p$  is illustrated in Fig. 7. The curves are plotted on the  $m$ - $\lambda$  plane in which  $\lambda$  is the normalized slenderness ratio defined by

$$\lambda = \frac{1}{\pi} \frac{L}{r} \sqrt{\epsilon_0} \dots\dots\dots(40)$$

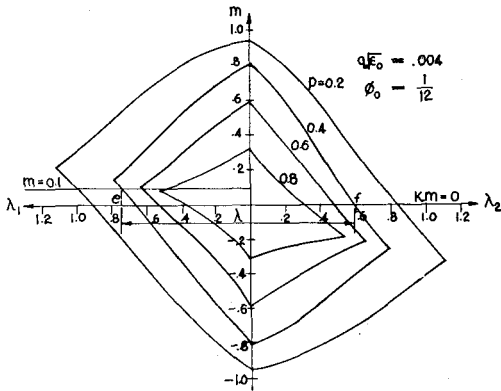


Fig. 7 Envelope of Equilibrium Curves.

It should be noted that the  $p-\lambda$  relation thus constructed for particular values of shear forces does not in general satisfy the static equilibrium condition as expressed by

$$Q = \frac{M(1-\kappa)}{L} \dots\dots\dots(41)$$

which can be nondimensionalized to the form

$$q = \frac{2\sqrt{2}m(1-\kappa)}{\pi^2\lambda} \dots\dots\dots(42)$$

The  $q\sqrt{\epsilon_0}-\lambda$  relationship given by Eq. (42) is plotted in Fig. 8 (c).

In order to determine the column curve which satisfies both the stability criterion and the static equilibrium condition, it has to be constructed from Figs. 8 (b) and 8 (c). For a certain value of  $\lambda$ , the corresponding value of  $q\sqrt{\epsilon_0}$  can be read from Fig. 8 (c). With the values of  $\lambda$  and  $q\sqrt{\epsilon_0}$  thus obtained, the value of  $p$  can readily be determined from Fig. 8 (b). Then the  $p-\lambda$  relationship or the column curve which satisfies both the stability criterion and static equilibrium can be plotted as illustrated in Fig. 8 (d).

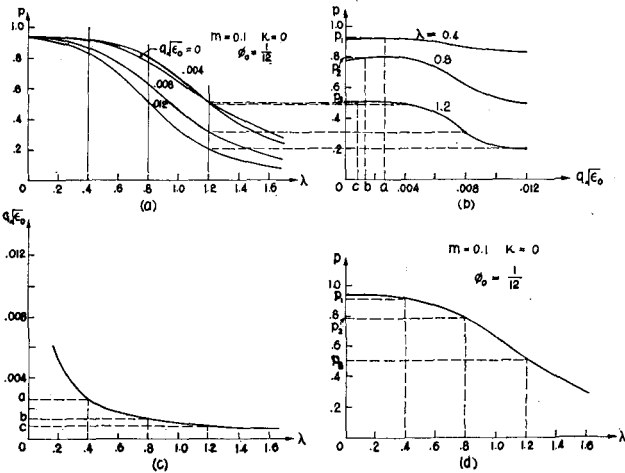


Fig. 8 Construction of Column Curves.

where  $L$  is the length of the column and  $r = a/\sqrt{2}$  is the radius of gyration of the cross section.

From envelopes such as the one shown in Fig. 7, the  $p-\lambda$  relationship can be constructed for specified values of end moment  $m$  and moment ratio  $\kappa$ . For example, the value of  $\lambda$  corresponding to  $p=0.4$  for  $m=0.1$  and  $\kappa=0$  can be read along the horizontal scale from point  $e$  to  $f$ . Similarly, the values of  $\lambda$  corresponding to different values of  $p$  can be obtained. The  $p-\lambda$  curves for various values of parameter  $q\sqrt{\epsilon_0}$  are plotted in Fig. 8 (a). From the  $p-\lambda$  curves thus obtained, the  $p-q\sqrt{\epsilon_0}$  relationships can be constructed by reading the corresponding values of  $p$  and  $q\sqrt{\epsilon_0}$  for particular values of  $\lambda$  as shown in Fig. 8 (b).

6. Discussions and Conclusions

For design purposes, the column curves are constructed for various values of  $m$  and  $\kappa$  as presented in Figs. 9 to 13. From these column curves, the moment-thrust interaction curves are also constructed and given in Figs. 14 to 18. By the virtue of nondimensionalization, the curves are applicable for various grades of structural steel.

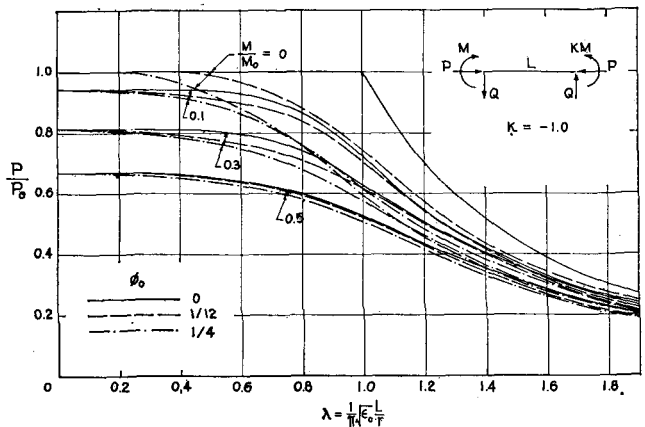


Fig. 9 Column Curve for  $\kappa = -1.0$ .

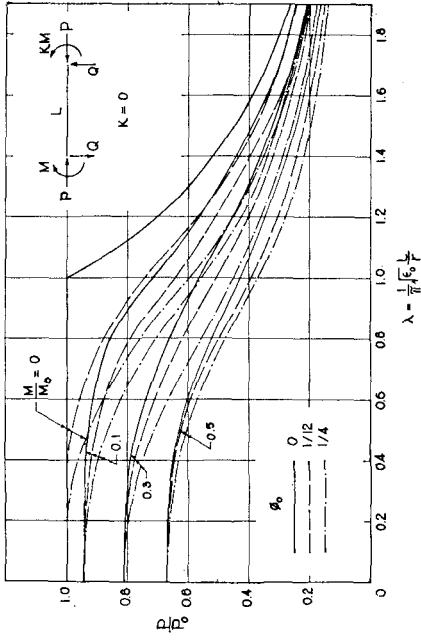


Fig. 10 Column Curve for  $\kappa = -0.5$ .

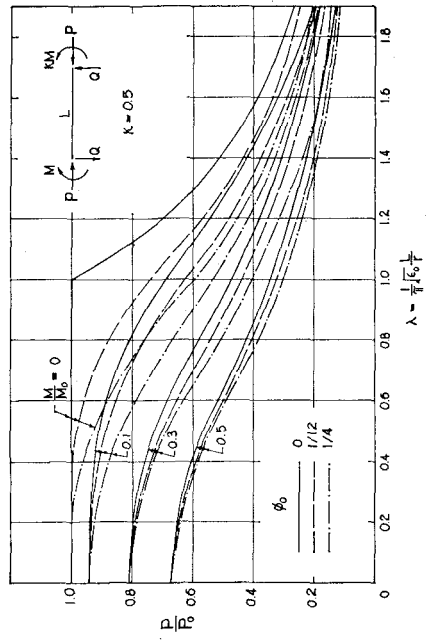


Fig. 11 Column Curve for  $\kappa = 0$ .

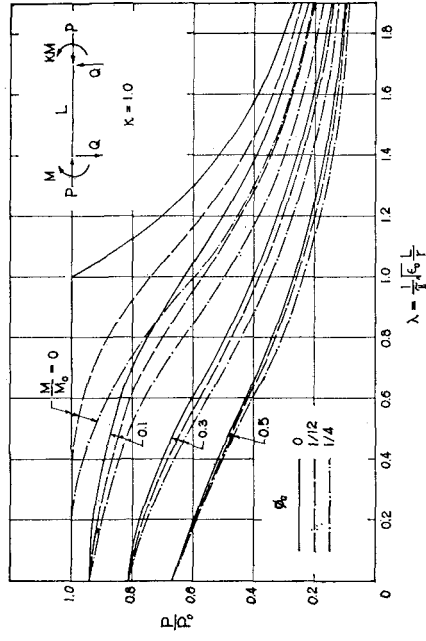


Fig. 12 Column Curve for  $\kappa = 0.5$ .

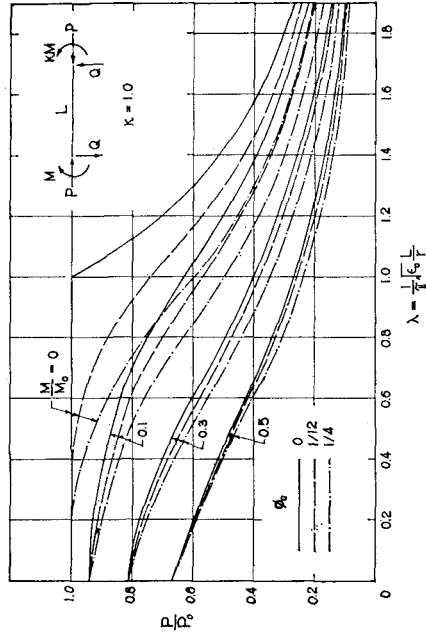


Fig. 13 Column Curve for  $\kappa = 1.0$ .

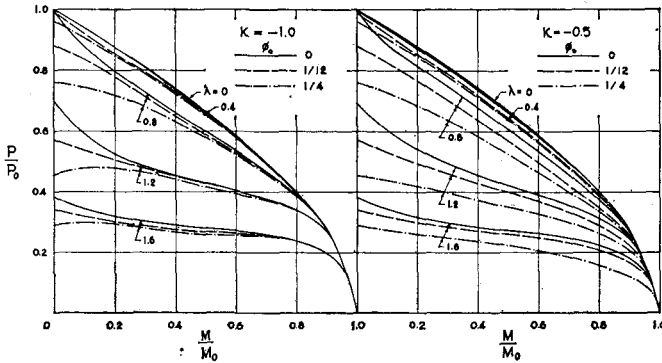


Fig. 14 *M-P* Interaction Curve for  $\kappa = -1.0$ .

Fig. 15 *M-P* Interaction Curve for  $\kappa = -0.5$ .

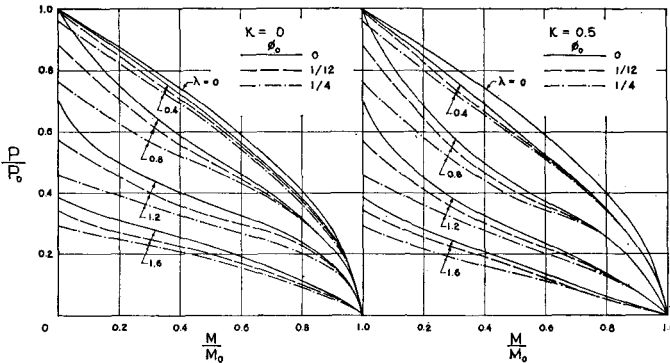


Fig. 16 *M-P* Interaction Curve for  $\kappa = 0$ .

Fig. 17 *M-P* Interaction Curve for  $\kappa = 0.5$ .

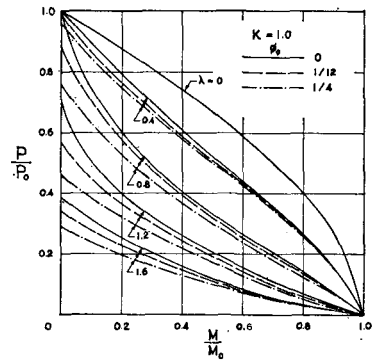


Fig. 18 *M-P* Interaction Curve for  $\kappa = 1.0$ .

The presence of initial imperfection generally reduces the strength of the otherwise straight columns. The effect of initial curvature is found to be more significant in the intermediate column range. The same fact was also reported by Batterman and Johnston<sup>8)</sup> and Nishino, Kanchanalai and Lee<sup>11)</sup>. It was also found from the numerical results that generally the effect of initial imperfection is greater for lower end moment  $M$  irrespective of the moment ratio  $\kappa$ . This effect tends to be diminished when the end moment is greater. From the moment-thrust interaction curves, it can be seen that columns under single curvature bending are normally weaker than those under double curvature bending.

REFERENCES

- 1) Von Karman, T.: "Die Knickfestigkeit gerader Staebе," *Phys. Z.*, Vol. 9, 1908, p. 136.
- 2) Baker, J. F., Horne, M. R., and Roderick,

- J. W.: "The Behavior of Continuous Stanchions," *Proceedings, Royal Society, London*, Vol. 198, 1949, p. 493.
- 3) Galambos, T. V., and Ketter, R. L.: "Columns Under Combined Bending and Thrust," *Journal of the Engineering Mechanics Division, ASCE*, Vol. 85, No. EM2, April, 1959, p. 1.
- 4) Horne, M. R.: "The Elastic-Plastic Theory of Compression Members," *Journal of Mechanics and Physics of Solids*, Vol. 4, 1956, p. 104.
- 5) Ellis, J. S.: "Plastic Behavior of Compression Members," *Journal of Mechanics and Physics of Solids*, Vol. 6, 1958, p. 282.
- 6) Lee, S. L., and Hauck, G. F.: "Buckling of Steel Columns Under Arbitrary End Loads," *Journal of the Structural Division, ASCE*, Vol. 90, No. ST2, April, 1964, p. 179.
- 7) Srichatrapimuk, T.: "Stability of Pipe Columns with Initial Curvature," *M. Eng. Thesis No. 354, Asian Institute of Technology*,

- Bangkok, Thailand, 1971.
- 8) Batterman, R. H., and Johnston, B. G.: "Behavior and Maximum Strength of Metal Columns," Journal of the Structural Division, ASCE, Vol. 93, No. ST2, April, 1967, p. 205.
  - 9) Rossow, E. C., Barney, G. B., and Lee, S. L.: "Eccentrically Loaded Steel Columns with Initial Curvature," Journal of the Structural Division, ASCE, Vol. 93, No. ST2, April, 1967, p. 339.
  - 10) Snyder, J., and Lee, S. L.: "Buckling of Elastic-Plastic Tubular Columns," Journal of the Structural Division, ASCE, Vol. 94, No. ST 1, January, 1968, p. 153.
  - 11) Nishino, F., Kanchanalai, T., and Lee, S. L.: "Ultimate Strength of Wide Flange and Box Columns," To be published in the Proceeding of Colloquium on Centrally Compressed Struts, Paris, November 1972.

*(Received July 15, 1972)*

---